Electronic Supplementary Information (ESI)

A smart rhodamine-pyridine conjugate for bioimaging of thiocyanate in living cells cells

Sandip Mandal,[a] Animesh Sahana,[a] Arnab Banerjee,[a] Damir A. Safin,*[b] Maria G. Babashkina,[b] Koen Robeyns,[b] Sjoerd Verkaart,[c] Joost G. J. Hoenderop,[c] Mariusz P. Mitoraj,*[d] Yann Garcia,*[b] and Debasis Das*[a]

[a]*Department of Chemistry, The University of Burdwan, 713104, Burdwan, West Bengal, India. Fax: (+91) 342 2530452; E-mail: ddas100in@yahoo.com*

[b]*Institute of Condensed Matter and Nanosciences, Molecules, Solids and Reactivity (IMCN/MOST), Université Catholique de Louvain, Place L. Pasteur 1, 1348 Louvain-la-Neuve, Belgium. Fax: +32(0) 1047 2330; Tel: +32(0) 1047 2831; E-mail: damir.a.safin@gmail.com, yann.garcia@uclouvain.be*

[c]*Department of Physiology, Radboud Institute for Molecular Life Sciences, Radboud University Medical Center, 6500 HB Nijmegen, The Netherlands*

[d]*Department of Theoretical Chemistry, Faculty of Chemistry, Jagiellonian University, R. Ingardena 3, 30-060 Cracow, Poland. E-mail: mitoraj@chemia.uj.edu.pl*

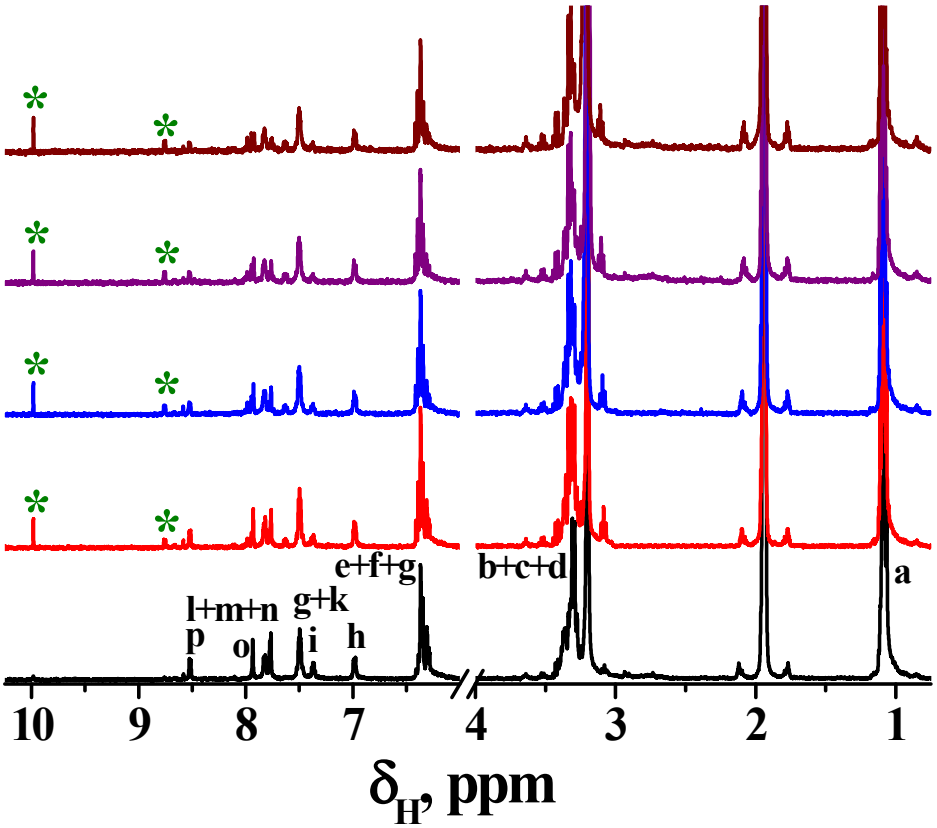

Fig. S1 ^{1}H NMR spectra of **REDA-2PC** (black), **REDA-2PC** + 0.5 equivalent of NCS^- (red), **REDA-2PC** + 1 equivalent of NCS^- (blue), **REDA-2PC** + 2.5 equivalents of NCS^- (purple) and **REDA-2PC** + 5 equivalents of NCS^- (wine) in CD_3CN:D_2O (9:1, v/v). For peak picking in the spectrum of **REDA-2PC** see Scheme S1. Some new bands are marked with an asterisk.

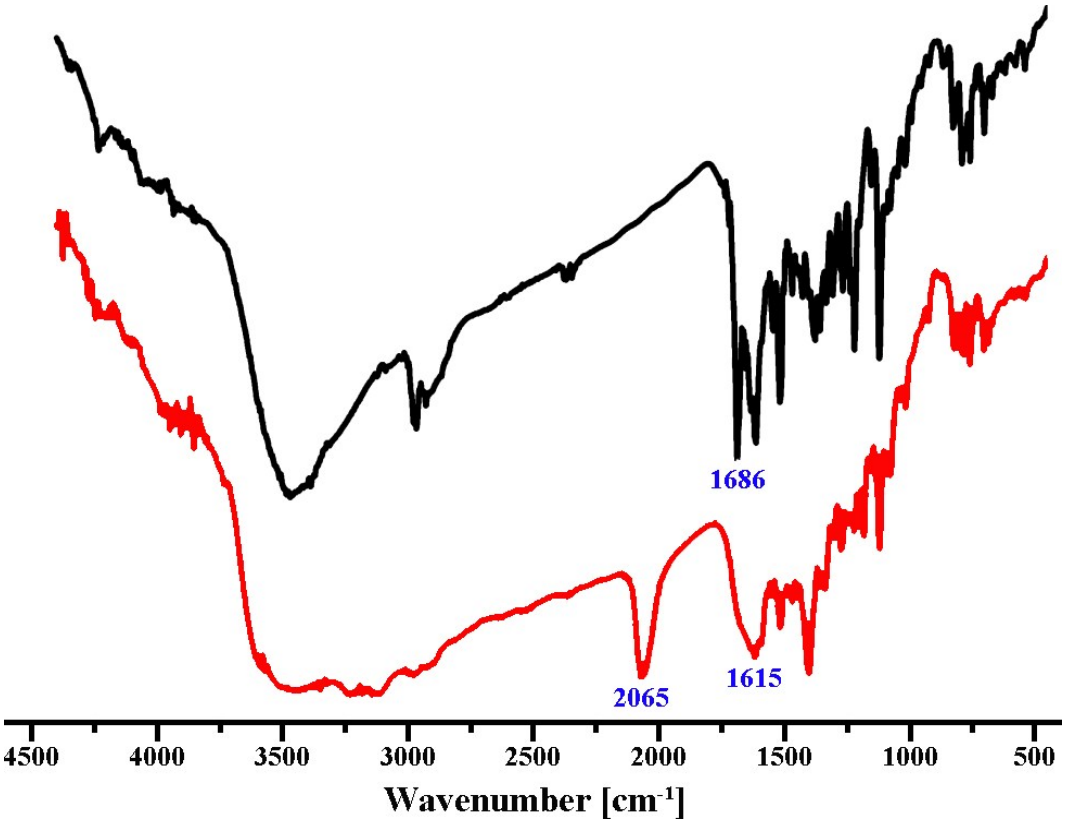

Fig. S2 FTIR spectra of **REDA-2PC** (black) and **[REDA-2PC + NCS⁻]** (red)

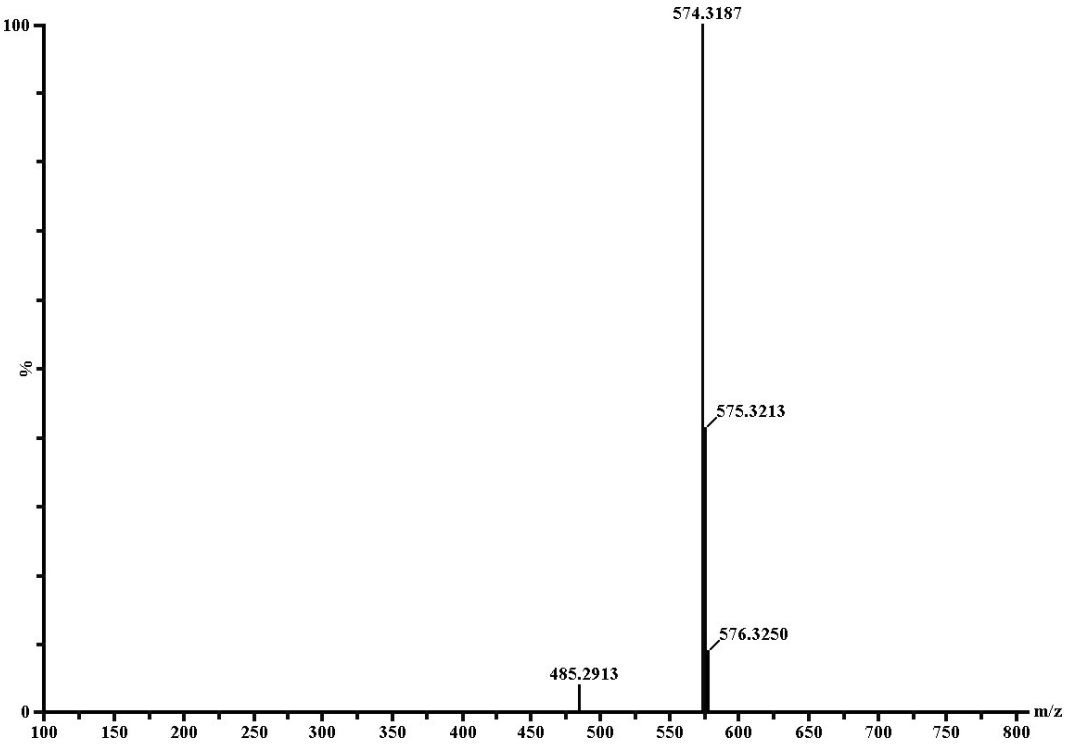

Fig. S3 The QTOF mass spectrum of **REDA-2PC**.

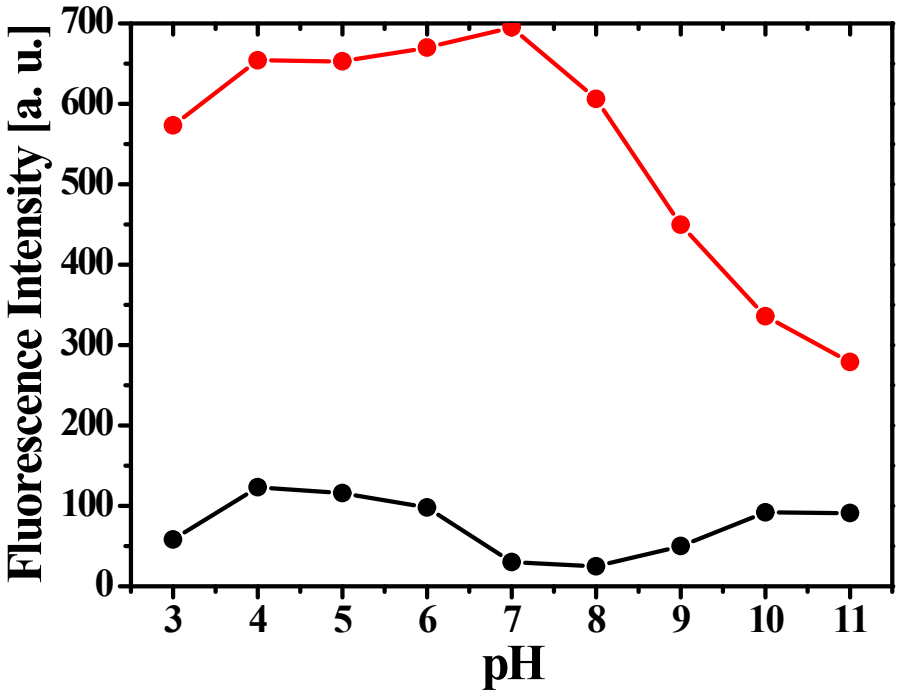

Fig. S4 Effect of pH on the emission intensity of **REDA-2PC** (black) and the [**REDA-2PC** + NCS^-] system (red).

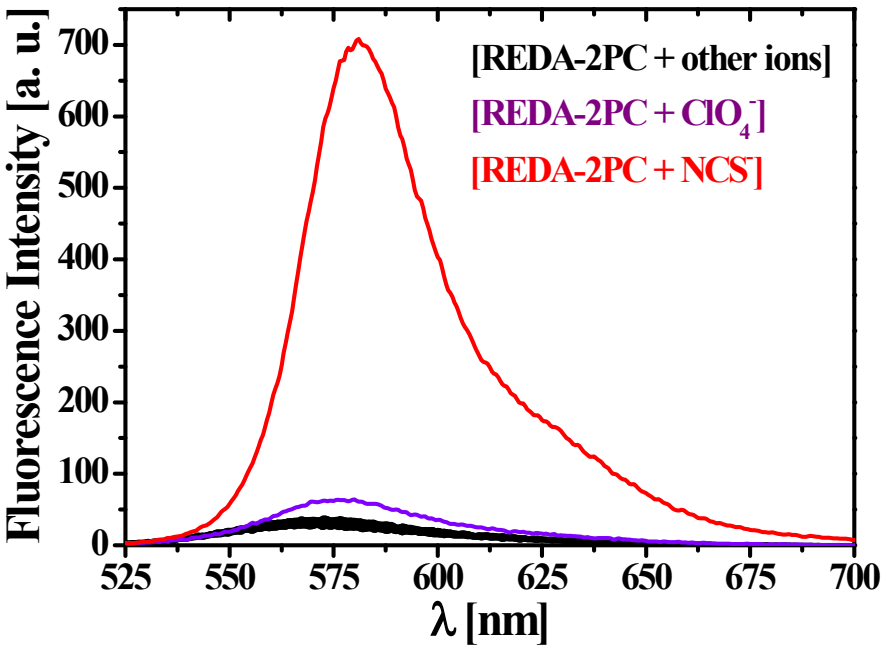

Fig. S5 Fluorescence spectra of **REDA-2PC** (50 μM) in HEPES buffered (0.1 M; CH_3CN:H_2O, 9:1 v/v; pH 7.4; λ_{exc} = 520 nm) solution in the presence of different anions: N_3^-, NO_2^-, NO_3^-, NCO^-, AcO^-, F^-, Cl^-, Br^-, I^-, SO_4^{2-}, $C_2O_4^{2-}$, $Cr_2O_7^{2-}$, PO_4^{3-}, AsO_4^{3-}, ClO_4^- and NCS^- (500 μM).

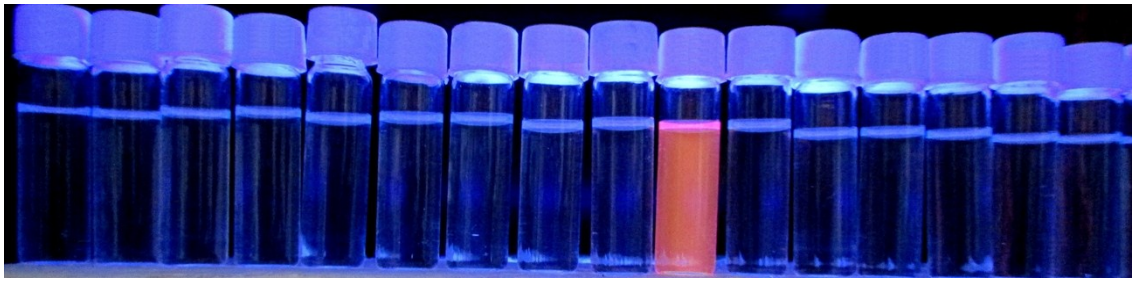

Fig. S6 UV light exposed colour of **REDA-2PC** (50 μM) in HEPES buffered (0.1 M; CH_3CN:H_2O, 9:1 v/v; pH 7.4) solution in the presence of 500 μM of different anions (from left to right: N_3^-, NO_2^-, NO_3^-, NCO^-, AcO^-, F^-, Cl^-, Br^-, I^-, NCS^-, SO_4^{2-}, $C_2O_4^{2-}$, $Cr_2O_7^{2-}$, PO_4^{3-}, AsO_4^{3-}, ClO_4^-).

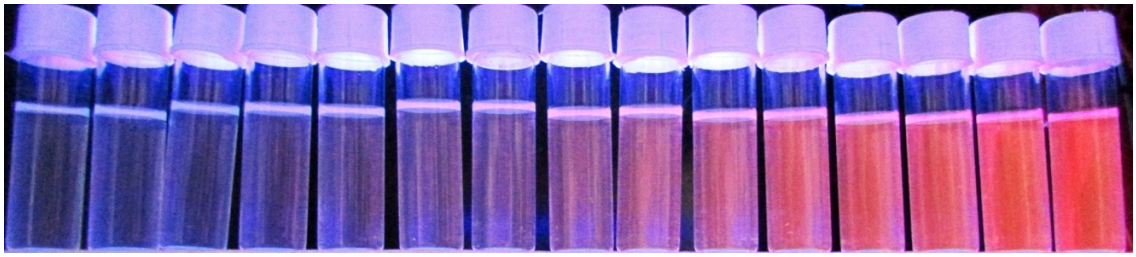

Fig. S7 UV light exposed colour of **REDA-2PC** (50 μM) in HEPES buffered (0.1 M; CH_3CN:H_2O, 9:1 v/v; pH 7.4) solution upon gradual addition of NCS^- (from left to right: 0, 0.001, 0.01, 0.1, 1.0, 3.0, 5.0, 7.0, 10.0, 25.0, 50.0, 75.0, 100.0, 250.0 and 500.0 μM).

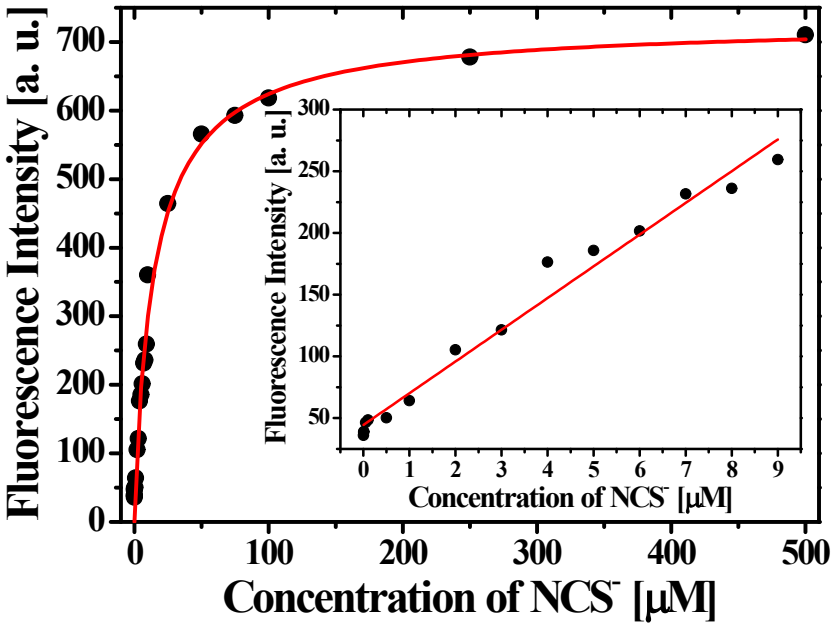

Fig. S8 Fluorescence intensity of **REDA-2PC** (50 μM) *vs.* externally added NCS^- (0.001–500 μM). Inset shows the linearity of the fluorescence intensity, observed up to 10 μM of added NCS^-.

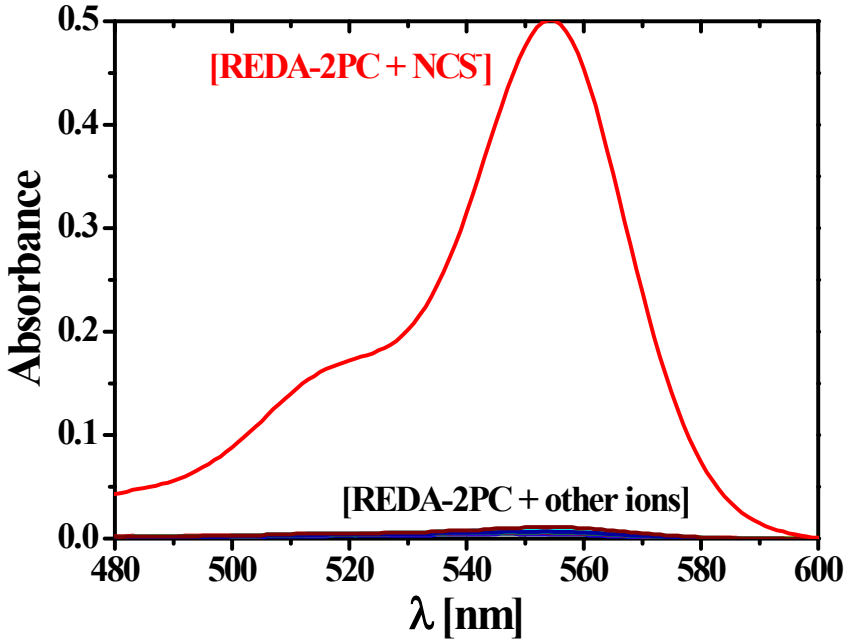

Fig. S9 Absorption spectra of **REDA-2PC** (50 μM) in HEPES buffered (0.1 M; CH_3CN:H_2O, 9:1 v/v; pH 7.4) solution in presence of different anions: N_3^-, NO_2^-, NO_3^-, NCO^-, AcO^-, F^-, Cl^-, Br^-, I^-, SO_4^{2-}, $C_2O_4^{2-}$, $Cr_2O_7^{2-}$, PO_4^{3-}, AsO_4^{3-}, ClO_4^- and NCS^- (500 μM).

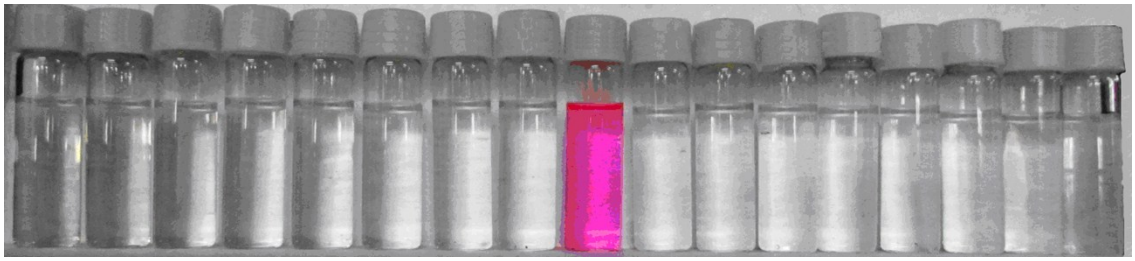

Fig. S10 Naked eye view of **REDA-2PC** (50 μM) in HEPES buffered (0.1 M; CH_3CN:H_2O, 9:1 v/v; pH 7.4) solution in presence of 500 μM of different anions (from left to right: only **REDA-2PC**, N_3^-, NO_2^-, NO_3^-, NCO^-, AcO^-, F^-, Cl^-, NCS^-, Br^-, I^-, SO_4^{2-}, $C_2O_4^{2-}$, $Cr_2O_7^{2-}$, PO_4^{3-}, AsO_4^{3-}, ClO_4^-).

Fig. S11 Naked eye view of **REDA-2PC** (50 μM) HEPES buffered (0.1 M; CH_3CN:H_2O, 9:1 v/v; pH 7.4) solution upon gradual addition of NCS^- (from left to right: 0, 0.001, 0.01, 0.1, 1.0, 3.0, 5.0, 7.0, 10.0, 25.0, 50.0, 75.0, 100.0, 250.0 and 500.0 μM).

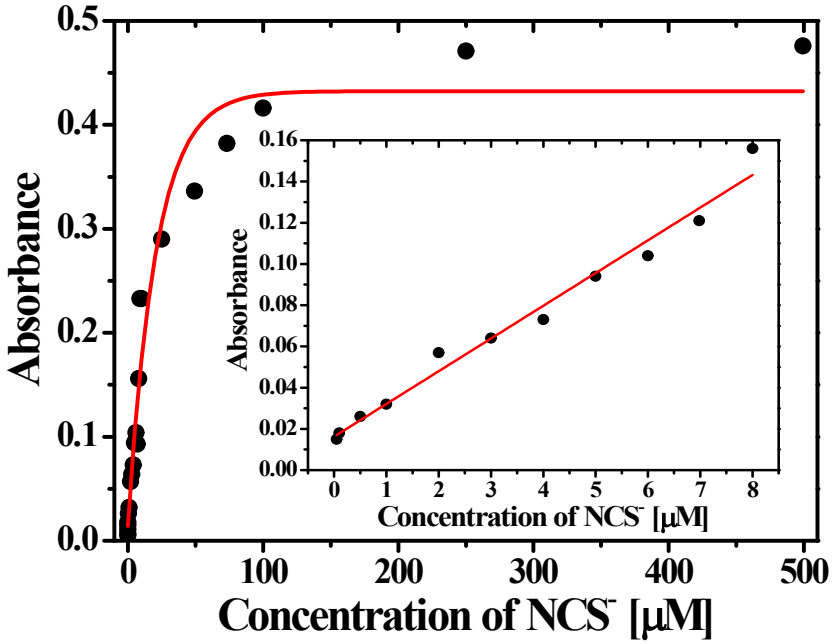

Fig. S12 Variation of absorbance of **REDA-2PC** (50 μM) at λ = 554 nm in HEPES buffered (0.1 M; CH_3CN:H_2O, 9:1 v/v; pH 7.4) solution as a function of externally added NCS^- (0.001–500 μM). Inset shows the linearity of the absorbance intensity, observed up to 10 μM of added NCS^-.

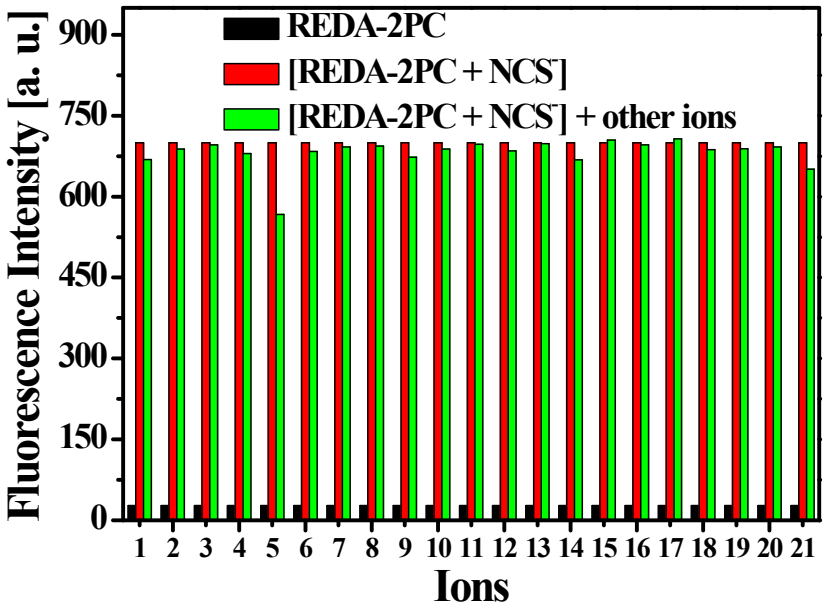

Fig. S13 Emission intensity of the [**REDA-2PC** (50 μM) + SCN^- (500 μM)] system in HEPES buffered (0.1 M; CH_3CN:H_2O, 9:1 v/v; pH 7.4; λ_{exc} = 520 nm) solution in presence of different ions (500 μM): N_3^- (1), NO_2^- (2), NO_3^- (3), NCO^- (4), AcO^- (5), F^- (6), Cl^- (7), Br^- (8), I^- (9), SO_4^{2-} (10), $C_2O_4^{2-}$ (11), $Cr_2O_7^{2-}$ (12), PO_4^{3-} (13), AsO_4^{3-} (14), ClO_4^- (15), Na^+ (16), K^+ (17), Mg^{2+} (18), Ca^{2+} (19), Fe^{3+} (20) and a mixture of all ions (21).

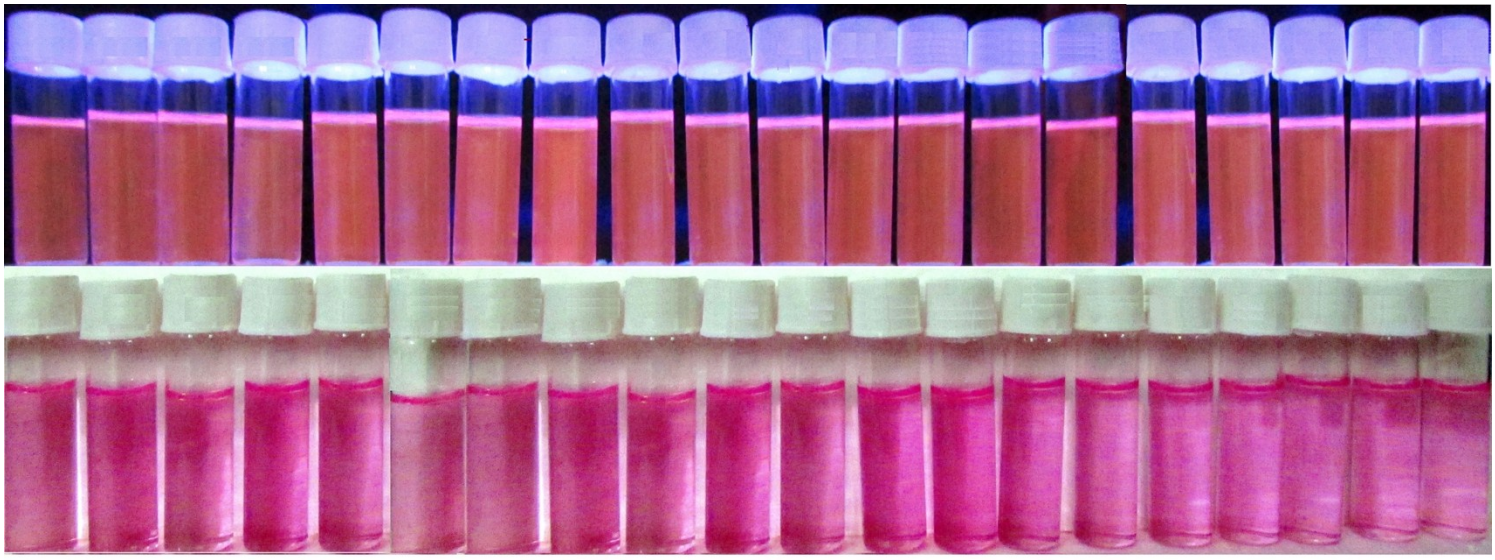

Fig. S14 Naked eye (bottom) and UV light exposed (top) views of the [**REDA-2PC** (50 μM) + SCN^- (500 μM)] system in HEPES buffered (0.1 M; $CH_3CN:H_2O$, 9:1 v/v; pH 7.4) solution in the presence of different ions (from left to right: N_3^-, NO_2^-, NO_3^-, NCO^-, AcO^-, F^-, Cl^-, Br^-, I^-, SO_4^{2-}, $C_2O_4^{2-}$, $Cr_2O_7^{2-}$, PO_4^{3-}, AsO_4^{3-}, ClO_4^-, Na^+, K^+, Mg^{2+}, Ca^{2+} and Fe^{3+}).

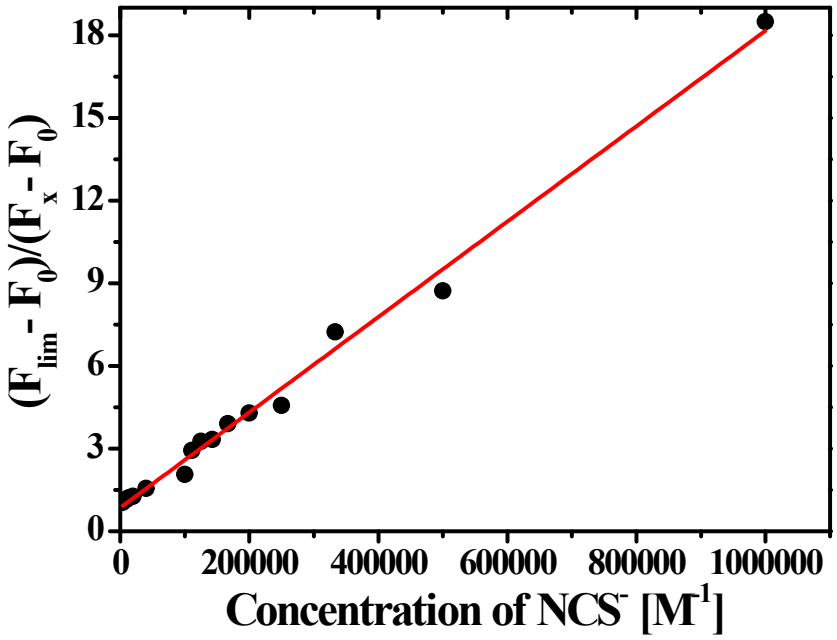

Fig. S15 Determination of the binding constant of **REDA** with NCS^- HEPES buffered (0.1 M; $CH_3CN:H_2O$, 9:1 v/v; pH 7.4; λ_{exc} = 520 nm) solution using $(F_{lim} - F_0)/(F_x - F_0) = 1 + (1/K) \times (1/[M]^n)$, where F_{lim}, F_0 and F_x are fluorescence intensities of **REDA** in the presence of NCS^- at saturation, free **REDA** and at any intermediate NCS^- concentration, respectively.

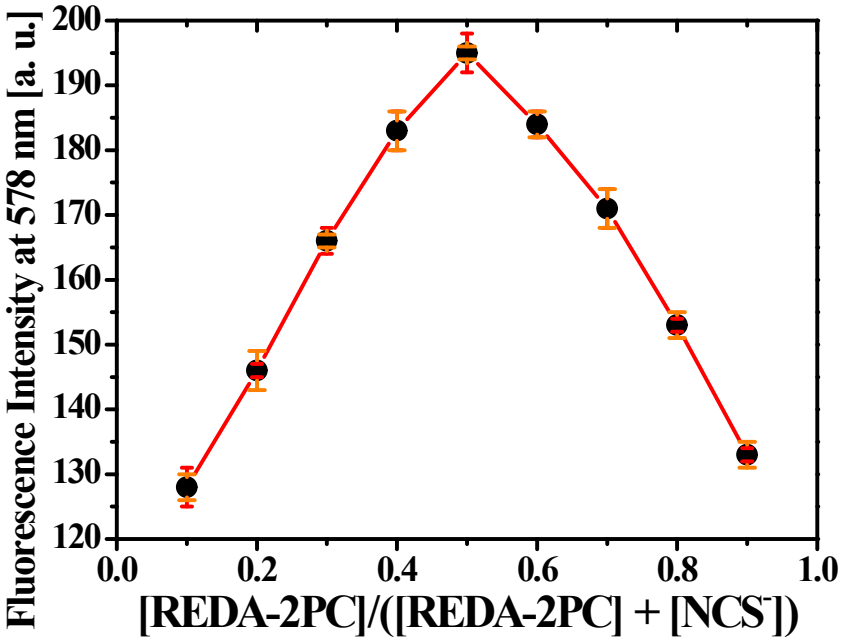

Fig. S16 Job's plot for the determination of stoichiometry of the [**REDA-2PC** (50 μM) + NCS^-] system in HEPES buffered (0.1 M; CH_3CN:H_2O, 9:1 v/v; pH 7.4) solution.

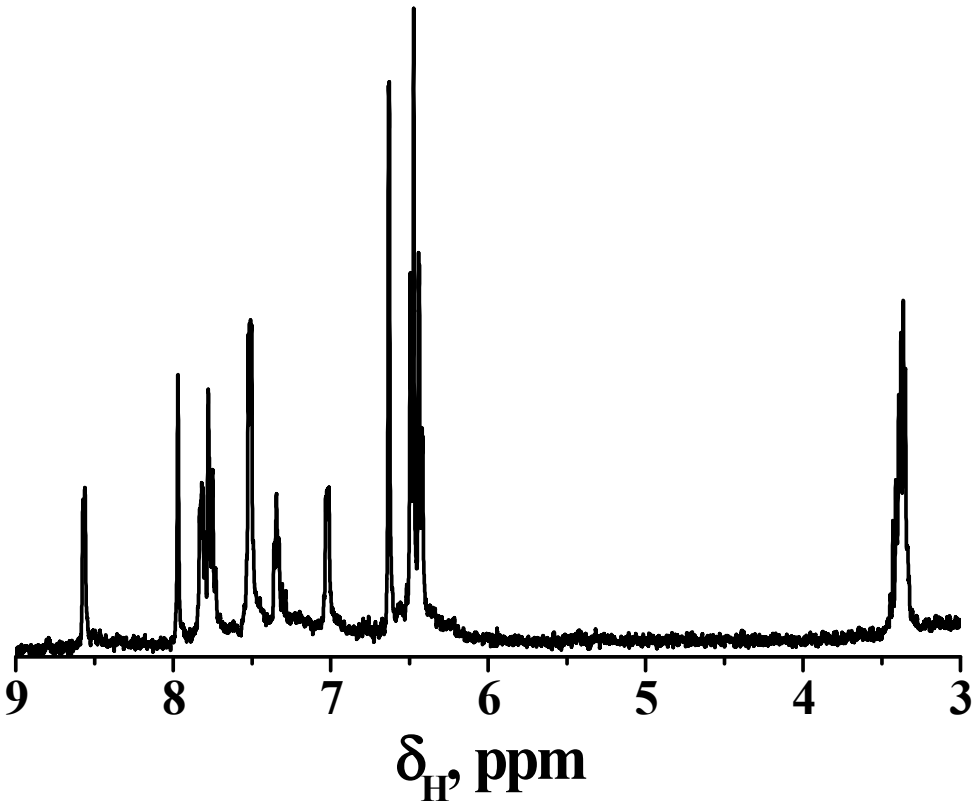

Fig. S17 ^1H NMR spectrum of **FEDA-2PC** in CD_3CN:D_2O (9:1, v/v)

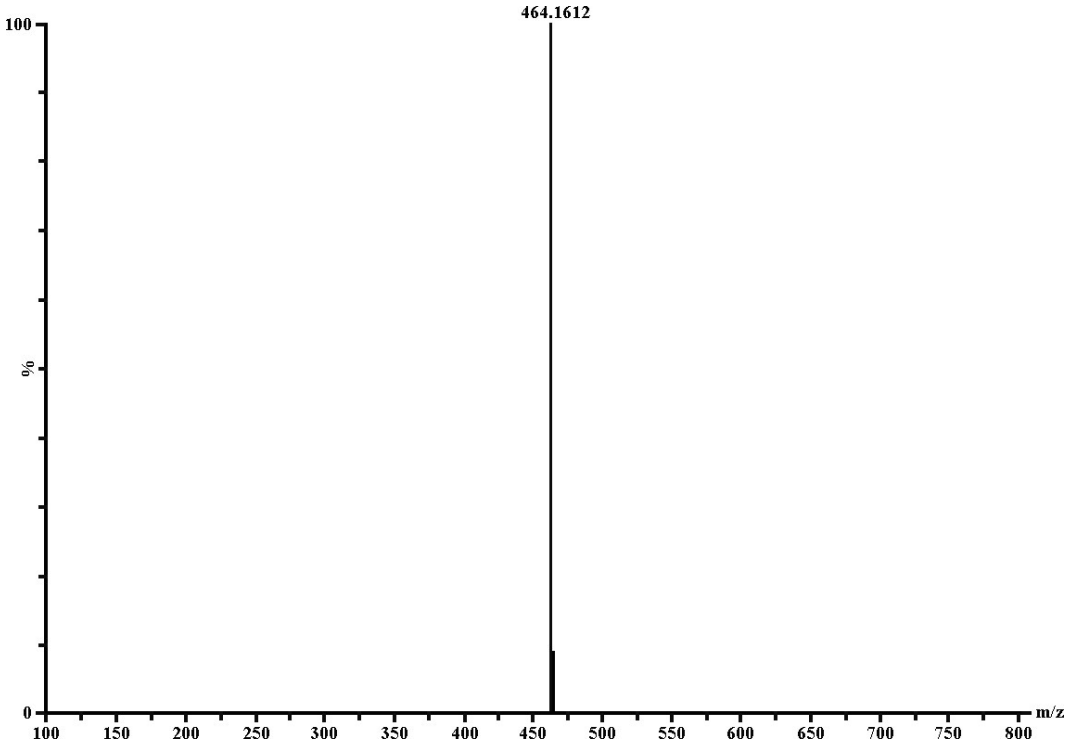

Fig. S18 The QTOF mass spectrum of **FEDA-2PC**.

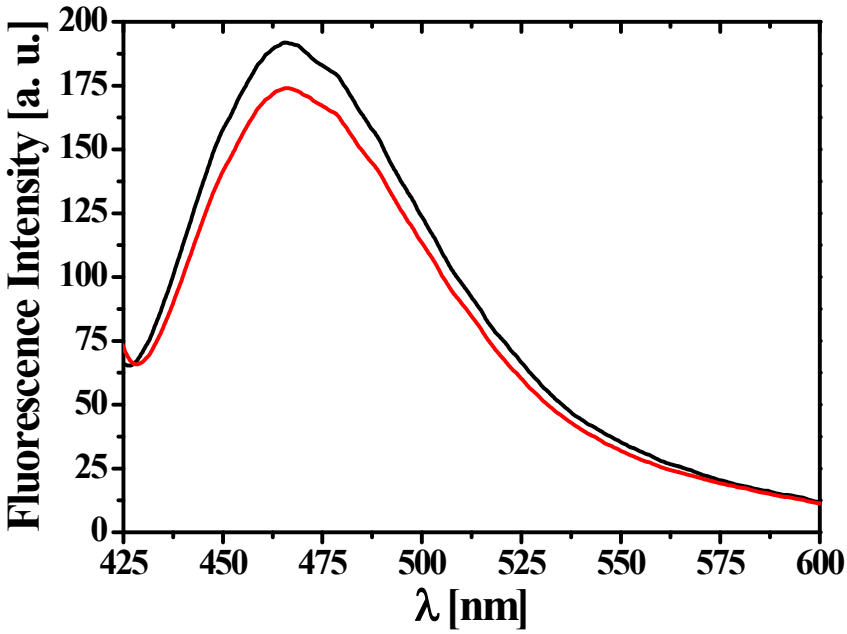

Fig. S19 Fluorescence spectra of **FEDA-2PC** (50 μM) in HEPES buffered (0.1 M; CH_3CN:H_2O, 9:1 v/v; pH 7.4; λ_{exc} = 405 nm) solution in absence (black) and presence (red) of NCS^- (500 μM).

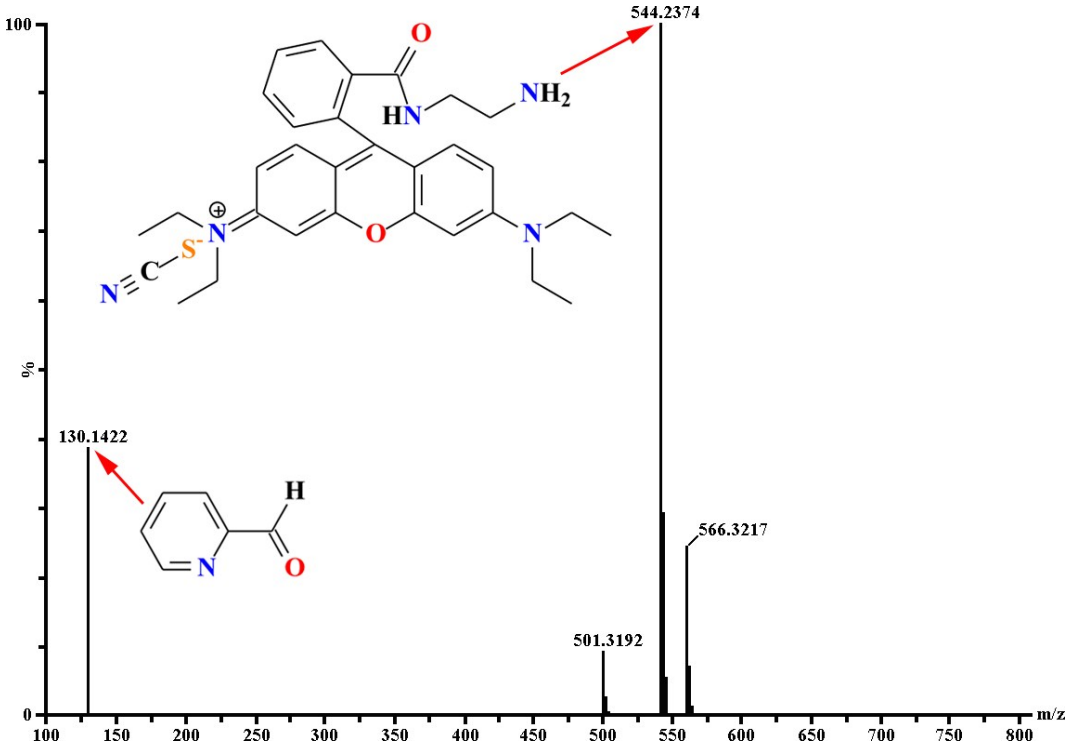

Fig. S20 The ESI mass spectrum of the species obtained after interaction of **REDA-2PC** with NCS^- in $CH_3CN:H_2O$ (9:1, v/v).

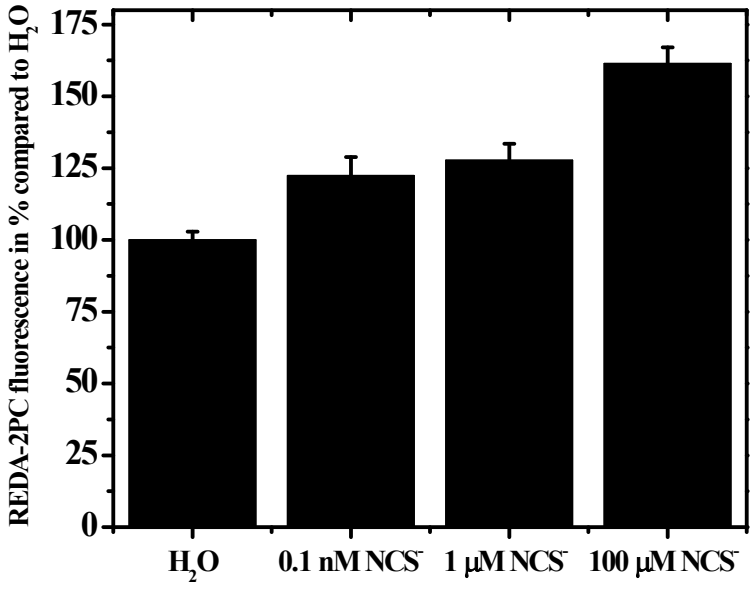

Fig. S21 Effect of the NCS^- incubation on the **REDA-2PC** (10 µM) fluorescence of human embryonic kidney 293 (HEK293) cells. Error bars represent mean + SEM of at least 90 cells per condition measured at three different days.

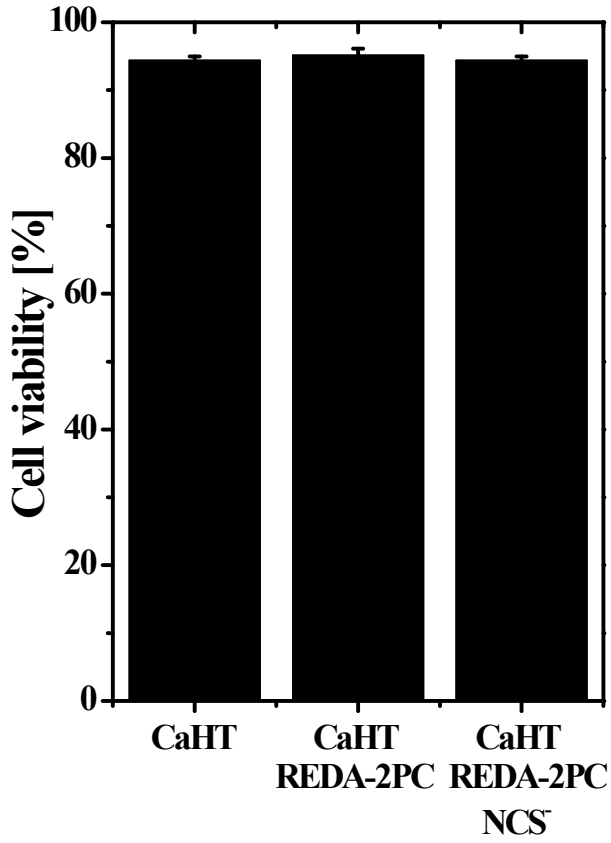

Fig. S22 Effect of **REDA-2PC** (10 µM) and **REDA-2PC** (10 µM) + NCS^- (100 µM) treatment on viability of HEK293 cells. Error bars represent mean + SEM of two experimental days of at least 206 cells per condition.

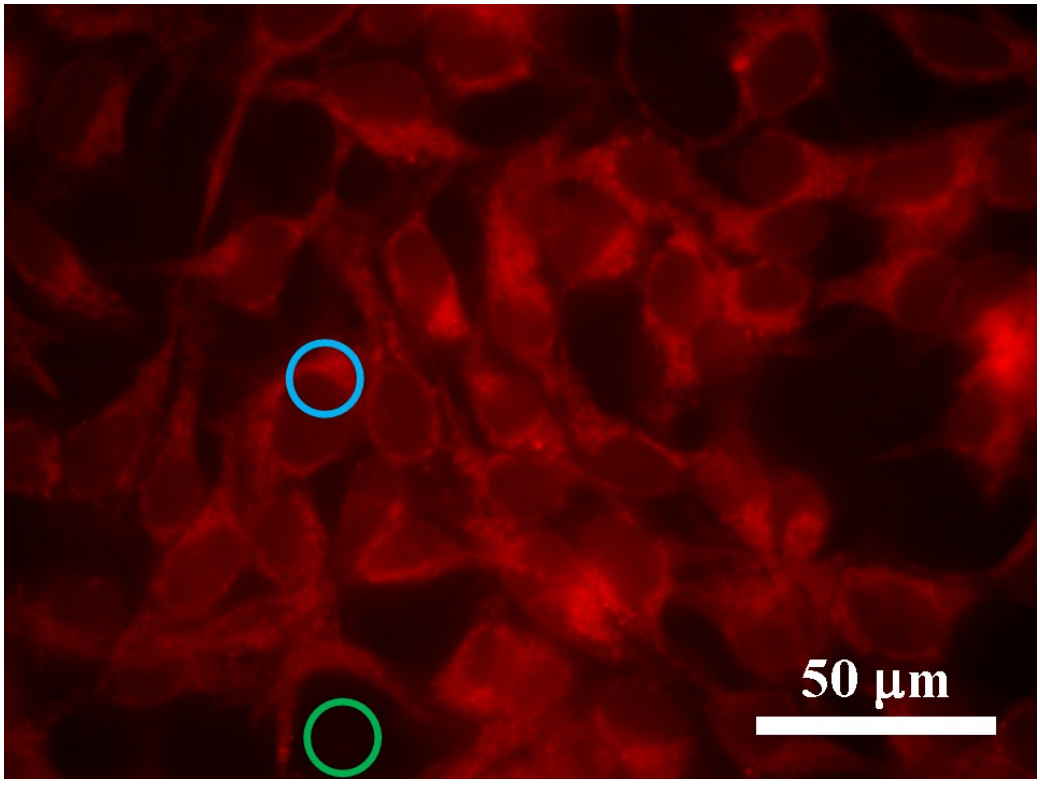

Fig. S23 Calculation of the intra-cellular NCS^- concentration.

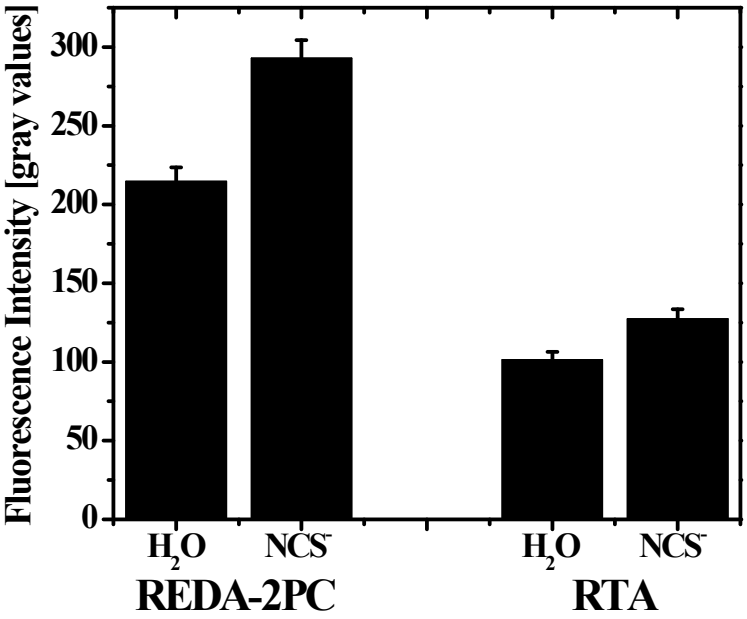

Fig. S24 Effect of NCS^- on the fluorescent intensities of **REDA-2PC** and **RTA**. Cells were treated as described in Fig. S22 with or without NCS^- (3 μM). Error bars represent mean + SEM of more than 40 individual cells measured at three different days.

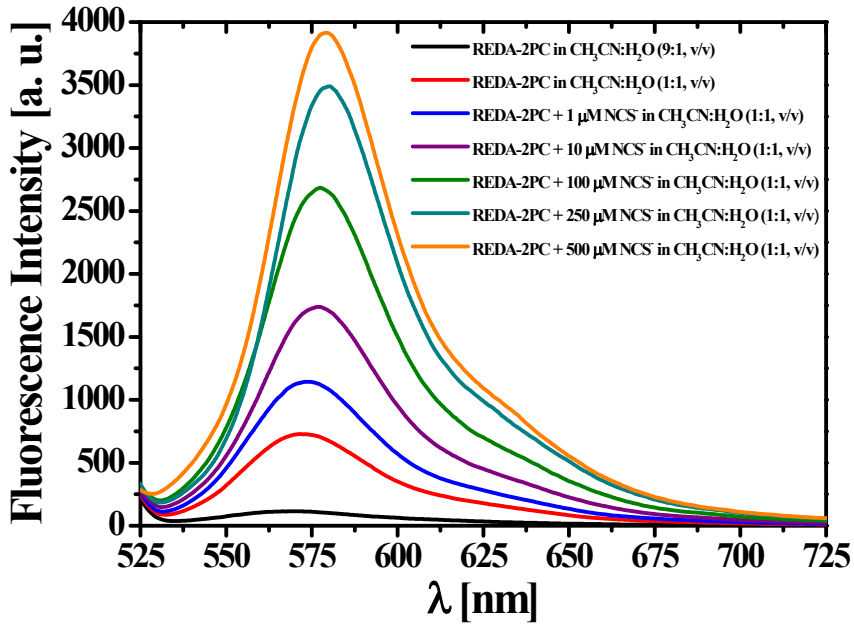

Fig. S25 Effect of the solvent composition on the emission intensities of **REDA-2PC** in the absence and presence of NCS^-.

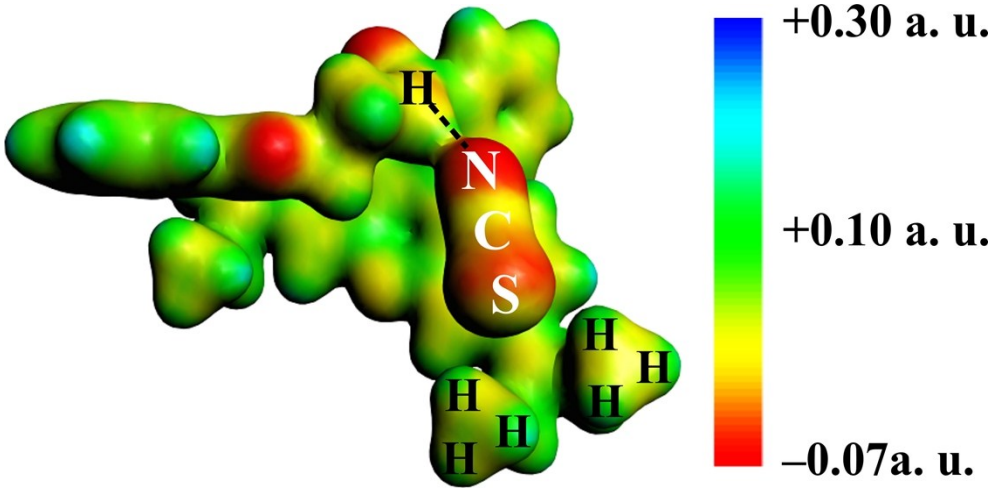

Fig. S26 Molecular electrostatic potential for the [**REDA-2PCH**]$^{+}$···**NCS**$^{-}$ complex, projected onto the electron density surface (0.002 a. u.).

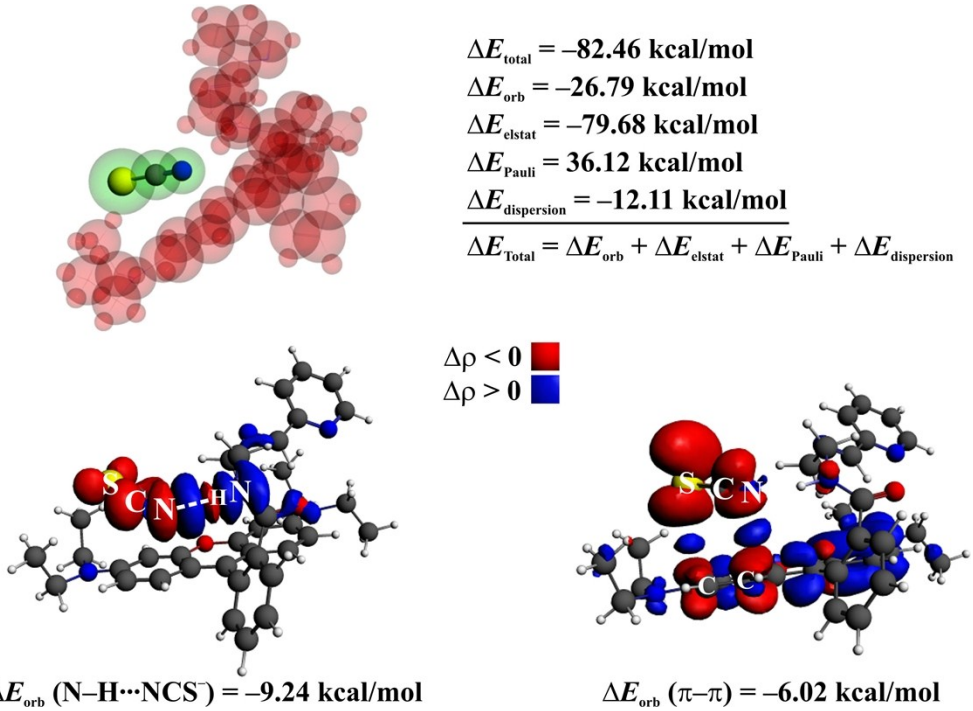

Fig. S27 The ETS energy decomposition (ADF/BLYP-D3/TZP) (top), and the most important NOCV-based deformation density channels, describing N–H···NCS^{-} (left bottom) and π–π stacking (right bottom) of **(1)[REDA-2PCH]**$^{+}$···**NCS**$^{-}$.

Table S1 Selected bond lengths (Å) and bond angles (°) for FEDA

Bond lengths					
N(25)–C(1)	1.487(3)	C(1)–C(17)	1.521(3)	C(12)–C(13)	1.369(3)
N(25)–C(23)	1.342(3)	C(2)–C(3)	1.391(3)	C(13)–C(14)	1.395(3)
N(25)–C(26)	1.454(3)	C(2)–C(7)	1.382(3)	C(17)–C(18)	1.383(3)
N(28)–C(27)	1.471(3)	C(3)–C(4)	1.375(4)	C(17)–C(22)	1.383(3)
O(8)–C(7)	1.380(3)	C(4)–C(5)	1.391(4)	C(18)–C(19)	1.383(3)
O(8)–C(9)	1.378(3)	C(5)–C(6)	1.381(3)	C(19)–C(20)	1.395(3)
O(15)–C(5)	1.360(3)	C(6)–C(7)	1.385(3)	C(20)–C(21)	1.380(3)
O(16)–C(11)	1.357(3)	C(9)–C(10)	1.391(3)	C(21)–C(22)	1.391(3)
O(24)–C(23)	1.246(3)	C(9)–C(14)	1.375(3)	C(22)–C(23)	1.476(3)
C(1)–C(2)	1.517(3)	C(10)–C(11)	1.385(3)	C(26)–C(27)	1.514(3)
C(1)–C(14)	1.512(3)	C(11)–C(12)	1.395(3)		
Bond angles					
N(25)–C(1)–C(2)	109.80(16)	O(16)–C(11)–C(12)	117.45(19)	C(9)–C(10)–C(11)	119.25(19)
N(25)–C(1)–C(14)	111.23(16)	O(24)–C(23)–N(25)	124.0(2)	C(9)–C(14)–C(13)	117.71(19)
N(25)–C(1)–C(17)	100.10(15)	O(24)–C(23)–C(22)	128.85(19)	C(10)–C(9)–C(14)	121.8(2)
N(25)–C(23)–C(22)	107.17(17)	C(1)–C(2)–C(3)	120.51(18)	C(10)–C(11)–C(12)	119.88(19)
N(25)–C(26)–C(27)	112.85(17)	C(1)–C(2)–C(7)	122.38(19)	C(11)–C(12)–C(13)	119.4(2)
N(28)–C(27)–C(26)	107.83(18)	C(1)–C(14)–C(9)	121.91(18)	C(12)–C(13)–C(14)	121.98(19)
C(1)–N(25)–C(23)	114.04(17)	C(1)–C(14)–C(13)	120.37(18)	C(14)–C(1)–C(17)	111.72(17)
C(1)–N(25)–C(26)	122.16(16)	C(1)–C(17)–C(18)	128.58(18)	C(17)–C(18)–C(19)	118.06(19)
C(23)–N(25)–C(26)	123.70(17)	C(1)–C(17)–C(22)	110.35(18)	C(17)–C(22)–C(21)	121.3(2)
C(7)–O(8)–C(9)	118.36(16)	C(2)–C(1)–C(14)	110.62(16)	C(17)–C(22)–C(23)	108.27(18)
O(8)–C(7)–C(2)	122.8(2)	C(2)–C(1)–C(17)	112.95(17)	C(18)–C(17)–C(22)	121.06(19)
O(8)–C(9)–C(10)	114.44(18)	C(2)–C(3)–C(4)	122.1(2)	C(18)–C(19)–C(20)	120.8(2)
O(8)–C(9)–C(14)	123.80(18)	C(3)–C(2)–C(7)	117.1(2)	C(19)–C(20)–C(21)	121.3(2)
O(15)–C(5)–C(4)	122.0(2)	C(3)–C(4)–C(5)	119.8(2)	C(20)–C(21)–C(22)	117.53(19)
O(15)–C(5)–C(6)	118.90(19)	C(4)–C(5)–C(6)	119.1(2)	C(21)–C(22)–C(23)	130.41(19)
O(16)–C(11)–C(10)	122.66(18)	C(5)–C(6)–C(7)	120.1(2)		

Table S2 Hydrogen bond lengths (Å) and angles (°) for FEDA[a]

D–H···A	*d*(D–H)	*d*(H···A)	*d*(D···A)	∠(DHA)
O(15)–H(15)···N(15)$^{\#1}$	0.84	1.88	2.721(3)	177
O(16)–H(16)···O(24)$^{\#2}$	0.84	1.81	2.630(2)	166
N(28)–H(28A)···O(15)$^{\#3}$	0.98(3)	2.30(3)	3.225(3)	158(2)
N(28)–H(28B)···O(24)$^{\#4}$	0.93(3)	2.50(3)	3.326(3)	149(2)

[a] Symmetry transformations used to generate equivalent atoms: #1 –1/2 + *x*, 3/2 – *y*, 1 – *z*; #2 *x*, –1 + *y*, *z*; #3 2 – *x*, 1 – *y*, 1 – *z*; #4 5/2 – *x*, –1/2 + *y*, *z*.

Table S3 Determination of the NCS^- concentration in diluted (40 times) sheep blood serum

Volume of the diluted blood serum (mL)	Fluorescence intensity (a. u.)	[NCS^-] found in free serum (μM)	Fluorescence intensity (a. u.) of serum after spiking 2 μM NCS^-	[NCS^-] found in serum after spiking 2 μM NCS^-
1.0	97.1	2.05 ± 0.01	148.6	4.07 ± 0.01
1.5	123.2	2.04 ± 0.01	175.3	4.06 ± 0.01
2.0	147.3	2.00 ± 0.01	198.6	4.04 ± 0.01

The NCS^- concentration found in sheep blood serum is 81.20 ± 0.01 μM.

Table S4 Determination of the NCS^- concentration in diluted (400 times) cow milk

Volume of the diluted blood serum (mL)	Fluorescence intensity (a. u.)	[NCS^-] found in free serum (μM)	Fluorescence intensity (a. u.) of serum after spiking 2 μM NCS^-	[NCS^-] found in serum after spiking 2 μM NCS^-
1.0	128.6	3.27 ± 0.01	179.9	5.31 ± 0.01
1.5	170.6	3.27 ± 0.01	223.2	5.32 ± 0.01
2.0	212.7	3.28 ± 0.02	265.3	5.30 ± 0.02

The NCS^- concentration found in cow milk is 1.31± 0.02 mM.